Genome-enabled discovery of evolutionary divergence in brains and behavior

Chinar Patil (cpatil6@gatech.edu)
Georgia Institute of Technology
Jonathan Sylvester
Georgia State University
Kawther Abdilleh
Georgia Institute of Technology
Michael W. Norsworthy
Catalog Technologies
Karen Pottin
Institut de Biologie Paris-Seine
Milan Malinsky
University of Basel
Ryan F. Bloomquist
Augusta University
Zachary V. Johnson
Georgia Institute of Technology
Patrick T. McGrath
Georgia Institute of Technology
Jeffrey T. Streelman
Georgia Institute of Technology

Research Article

Keywords: Malawi Cichlids, genome sequencing, evolutionary reverse genetics, brain development, behavior

Posted Date: March 12th, 2021

DOI: https://doi.org/10.21203/rs.3.rs-275291/v1

Genome-enabled discovery of evolutionary divergence in brains and behavior

Chinar Patil[*1], Jonathan B. Sylvester[1,2], Kawther Abdilleh[1], Michael W. Norsworthy[3,4], Karen Pottin[5], Milan Malinsky[6,7], Ryan F. Bloomquist[1,8], Zachary V. Johnson[1], Patrick T. McGrath[1], Jeffrey T. Streelman[1]

Affiliations:
[1]School of Biological Sciences and Petit Institute of Bioengineering and Bioscience, Georgia Institute of Technology, Atlanta, GA, USA.
[2]Department of Biology, Georgia State University, Atlanta, GA, USA
[3]Catalog Technologies Inc., Boston, MA, USA.
[4]Freedom of Form Foundation, Inc., Cambridge, MA, USA.
[5]Laboratoire de Biologie du Dévelopement (IBPS-LBD, UMR7622), Sorbonne Université, CNRS, Institut de Biologie Paris Seine, Paris, France.
[6]Zoological Institute, Department of Environmental Sciences, University of Basel, Basel, Switzerland.
[7]Wellcome Trust Sanger Institute, Cambridge, United Kingdom.
[8]Augusta University, Department of Oral Biology and Diagnostic Sciences, Department of Restorative Sciences, Dental College of Georgia, Augusta, GA, USA.

Corresponding Author:
Chinar Patil
Email: cpatil6@gatech.edu

Keywords: Malawi Cichlids, genome sequencing, evolutionary reverse genetics, brain development, behavior

Abstract

Lake Malawi cichlid fishes exhibit extensive divergence in form and function built from a relatively small number of genetic changes. We compared the genomes of rock- and sand-dwelling species and asked which genetic variants differed among the groups. We found that 96% of differentiated variants reside in non-coding sequence but these non-coding diverged variants are evolutionarily conserved. Genome regions near differentiated variants are enriched for craniofacial, neural and behavioral categories. Following leads from genome sequence, we used rock- vs. sand- species and their hybrids to (i) delineate the push-pull roles of BMP signaling and *irx1b* in the specification of forebrain territories during gastrulation and (ii) reveal striking context-dependent brain gene expression during adult social behavior. Our results demonstrate how divergent genome sequences can predict differences in key evolutionary traits. We highlight the promise of evolutionary reverse genetics – the inference of divergence in phenotype from genome sequencing in natural populations.

Introduction

Our understanding of how the genome encodes natural variation in form and function is still limited. This is the case for almost any trait, from height to behavior to complex disease [1]. The reasons for this are manifold, but they include an underappreciated role of non-coding genetic variants linked to differences in traits. This is apparent in our assumptions and in syntheses of data. For instance, only 25 years ago, experts thought that the human genome might contain 70,000 to over 100,000 genes to account for our complexity [2]. More recently, it has been estimated that upwards of 93% of human disease related variants – traits for which we have the most data from genome wide association studies (GWAS) – reside in noncoding DNA sequence [3]. Many of these noncoding variants are regulatory, that is, they affect the expression of genes [4]. Therefore, despite a refined understanding of how single genes work in controlled cellular environments, it remains unclear how the genome is activated to produce natural phenotypes, and this may be particularly vexing for context-dependent processes like development or behavior.

Over the past two decades, systems have been developed to identify the genetic basis of traits from nature [5]. Amongst vertebrate animals, these traits include body armor [6], color [7], head and jaw shape [8-10], parental care [11,12], song [13] and coordinated movement [14]. The take home message from this work has been that a small number of genes from recognizable pathways explain a considerable proportion of phenotypic variance. Yet, these studies may be biased in interpretation and limited in inference space. The focus is typically on one or two species and one trait at a time, often using hybrid pedigrees founded by a small number of individuals, and candidate gene or QTL approaches. Here, we explored a different strategy in a system of many species with many divergent traits. We sought to determine the genetic differences between closely related groups of species and then to focus experiments on leads from genome divergence. In essence, we've asked the genome which traits to follow.

The Malawi cichlid system is an apposite one for our research aims. The assemblage comprises hundreds of closely related species that have diversified in the last 500,000 to

one million years [15], such that the genomes of individuals across species boundaries remain highly similar [16]. An appreciable fraction of genetic polymorphism identified in Malawi species is shared with cichlid lineages from throughout East Africa -- suggesting that ancient genetic variation fuels diversification of the Malawi flock [17]. Set against this background of genome similarity, Malawi cichlids exhibit staggering diversity in phenotypes including pigmentation [18], sex determination [19,20], craniofacial and brain patterning [8,21,22] and social behavior [23-25]. Previous work has focused on the genomic and early developmental underpinnings of this diversity, in rock- *vs*. sand-dwelling species [16,21,22,26].

Rock- vs. sand- species form ecologically distinct groups similar to other ecotypes in well-known adaptive radiations (marine *vs*. freshwater sticklebacks; tree *vs*. ground finches and anoles) [27]. The main difference in this case is that each of the rock- and sand- groups contains more than 200 species. Recent divergence, rapid speciation and meta-population dynamics synergistically lead to the broad sharing of polymorphism across the rock-sand speciation continuum [17,28]. Malawi rock-dwellers tend to be strongly territorial and aggressive; they breed and feed at high density in complex rock-reef habitats. Most eat algae from the substratum with strongly reinforced jaws packed with teeth. Adult rock-dweller brains exhibit enlarged anterior components, telencephala and olfactory bulbs. Sand-dwellers are less site-specific and less aggressive. They often breed on communal leks where males build sand 'bowers' to attract females [29]. Many capture small prey using acute vision and fast-moving gracile jaws; their brains and sensory apparatus are elaborated for more posterior structures optic tecta, thalamus and eyes (Supplementary Figure 1). We aimed to understand evolutionary divergence between rock- and sand-dwelling lineages by identifying the number, type and spectrum of genetic variants that separate these groups.

To target this primary axis of evolutionary divergence in the Lake Malawi species assemblage [27], we compared whole genomes of one male individual each from 8 rock-dwelling and from 14 sand-dwelling species (Supplementary Table 1), to an average of 25X coverage per individual. Species were chosen to represent the diversity present

within each of the rock- and sand- groups (Figure 1A), in terms of body size, color pattern, ecology and phylogenetically defined lineages within the sand- species group [28].

Results

The genomic signature of rock-sand divergence

We compared the genomes of 8 rock dwellers and 14 sand dwellers to uncover the genomic signature of rock- versus sand- evolutionary diversification. We aligned sequence data to a reference genome of nearly 1 gigabase [30] and identified approximately 22 million Single Nucleotide Polymorphisms (SNPs) and 200,000 Insertion-Deletions (InDels). We calculated F_{ST} per variant, and averaged across 10kb windows, to quantify divergence between rock and sand species. We found that 0.06% of SNPs and 0.44% of InDels are alternately fixed between rock- and sand- groups. When these divergent variants and genome regions (2.5% FDR) are mapped to linkage groups (chromosomes), it is apparent that the signature of rock- vs. sand- divergence is distributed relatively evenly across the chromosomes (Figure 1B). Among fixed variants, 3.5% were found in coding regions and 96.5% were predicted to be non-coding; ~17% in intergenic regions, 38% in introns, 38% in flanking regions (within 25kb up- or downstream of a gene), and 3% in annotated UTRs. Rock vs. sand fixed coding variants were more likely to be missense/loss-of-function (72.6%) than silent (27.3%).

We next generated whole-genome alignments of five published cichlid reference genomes from across East Africa [31] and estimated an evolutionary conservation score for each nucleotide position. Akin to phylogenetic footprinting, this approach allows inference of function for regions that are slower to change than others due to the long-term effect of purifying selection. For both coding and non-coding portions of the genome, we found that rock-sand divergence correlates positively with evolutionary conservation scores (Figure 1C), suggesting that differentiated rock-sand variants, including many non-coding variants, are enriched for function.

A total of 4,484 genes lie within 25 kb of either an alternately fixed variant or a highly divergent 10kb window (2.5%FDR). Pathway enrichment analysis [32] of human homologs/analogs for these genes reveals categories spanning early embryonic development, craniofacial morphogenesis, brain development, synaptic transmission and

neuronal function (Supplementary Table 2). In particular, rock-sand divergent genes are enriched for GO Biological Process terms ‘telencephalon development’ ($p < 1.7e-18$), ‘adult behavior’ ($p < 2e-14$), ‘synaptic plasticity’ ($p < 1.4e-12$), ‘odontogenesis’ ($p < 3.7e-11$), ‘response to BMP’ ($p < 3.2e-09$), ‘gastrulation’ ($p < 5.6e-06$), ‘face morphogenesis’ ($p < 8.9e-08$), ‘neural crest cell differentiation’ ($p < 4.3e-13$), and ‘eye development’ ($p < 1.3e-15$). Over-represented gene families included nuclear hormone receptors ($p < 3.0e-08$), HOXL subclass homeoboxes ($p < 1.4e-07$), TALE class homeoboxes ($p < 4.2e-04$) and Forkhead boxes ($p < 9.33-04$; for novel expression domains in cichlid *foxp2* see Supplementary Figure 2). We observed enrichment for the mouse phenotypes ‘abnormal cognition’ ($p < 3.3e-15$), ‘abnormal learning and memory’ ($p < 2.6e-15$), ‘abnormal craniofacial morphology’ ($p < 4.9e-11$) and ‘abnormal social/conspecific interaction’ ($p < 7.1e-14$). We used the list of differentiated genes to query an Allen Brain Atlas dataset that reports gene expression in hundreds of brain regions [33]. Rock- sand- divergent genes were enriched for the basomedial nucleus of the amygdala, a sub-region of the telencephalon ($p_{adj} = 0.001$) that regulates fear, anxiety, and physiological responses to territorial intruders in rodents [34,35], and has been linked to Social Anxiety Disorder in humans [36]. Finally, we queried databases of genes involved in human disease. Genes near divergent variants are significantly enriched for factors implicated in neurological disease like Autism Spectrum Disorder (SFARI [37], Fisher’s exact test p value < 2e-16) and disorders related to the neural crest [38], (Fisher’s exact test p value < 2e-16).

Given the prevalence of evolutionarily conserved, non-coding, divergent rock-sand variants and genome-wide enrichment for craniofacial and neural crest biology, we examined overlap with published datasets of mammalian neural crest and craniofacial enhancers [39,40]. These data allow us to identify craniofacial and cranial neural crest cell (CNCC) enhancers conserved between mammals and cichlids and fixed variants between rock and sand species within these conserved regulatory elements. A total of 275 craniofacial enhancer elements and 234 human CNCC enhancers are evolutionarily conserved between mammals and cichlids. We found divergent rock-sand mutations within the enhancer elements of key genes integral to CNCC specification and migration (Supplementary Table 2). Notably, from both datasets, fixed rock-sand variants were

found within the enhancer region of the gene *nr2f2*, a nuclear receptor and master neural crest regulator [41]. Rock-sand divergent variants were similarly located within craniofacial enhancers of three genes (*yap1*, *fat4*, *rere*) that function in the Hippo signaling pathway, as well as within enhancers of *irx3* and *axin2*. These data linking rock-sand fixed SNP/InDels to evolutionarily conserved, experimentally verified enhancers further underscore the importance of non-coding variation in the craniofacial evolution of rock- and sand- lineages [42].

Genome-wide divergence between rock vs. sand Malawi cichlids involves a relatively small percentage of genetic variants. Divergent variants are (a) predominantly non-coding, (b) in long-term evolutionarily conserved loci (c) enriched for genes and pathways involved in embryonic development, brain development, brain function and behavior, and craniofacial morphogenesis. Given these strong patterns of enrichment, we used the experimental power of the Malawi cichlid system to interrogate features of early development and adult behavior that differ between rock- and sand- groups.

A gastrula-stage map of forebrain diversification

Rock- vs. sand-dwelling Malawi cichlids exhibit divergence in or near genes enriched for BMP signalling, gastrulation, eye and telencephalon development, as well as the TALE (Irx) gene family. To explore the developmental consequences of this differentiation, we investigated early forebrain specification in rock- and sand- embryos, building upon our previous studies and interest in *irx1b* and early brain development [21,22]. During development, the complexity of the vertebrate brain is first laid out in the neural plate, a single-cell thick sheet of cells that forms between non-neural ectoderm and the germ ring at gastrulation. Irx genes act as transcriptional repressors of BMP signal in gastrulation, and function to specify the neural plate [43]. BMPs, in turn, are protective of the anterior-most region of the neural plate, which will ultimately give rise to the telencephalon, and suppress the eye field [44]. Given alternatively fixed variants in the *irx1b* gene, expected interactions between Irx and BMP signaling in the early embryo and known telencephalon

197 vs. eye size differences between rock- vs. sand- species [21,22], we examined and
198 quantified the early activity of *irx1b* and BMP in rock- vs. sand- embryos.
199
200 We used a custom device to orient and image cichlid embryos *in toto* at gastrula and
201 neurula stages [45]. In early gastrula (EG), *irx1b* (red) and BMP signal (green, PSMAD)
202 delineate complementary dorsal and ventral domains of the embryo (Figure 2A). By mid-
203 gastrula (MG), *irx1b* shows two expression domains, one in the posterior portion of the
204 developing neural plate (np) and the second co-expressed with PSMAD activity around
205 its anterior border (white arrowheads). By late gastrula (LG), the domains of *irx1b*
206 expression and PSMAD activity sharpen around the leading edge of the neural plate but
207 remain overlapping around the periphery. Notably, *irx1b* expression is expanded in the
208 anterior domain of sand-dwellers (S) compared to rock-dwellers at EG and MG, and then
209 defines the boundary of the neural plate earlier in sand-dwellers (S) in LG (arrowheads).
210 As a consequence, BMP signal should have a longer-lasting influence on the neural plate
211 in rock-dwelling species. Based upon manipulative experiments in zebrafish [44], this is
212 predicted to result in a relatively larger presumptive telencephalon and smaller eye field.
213
214 We developed a panel of rock- x sand- hybrid crosses to formally evaluate the role of
215 *irx1b* in forebrain diversification. First, we used quantitative RT-PCR to measure allele-
216 specific expression (ASE) in heterozygous rock- x sand- F_2 hybrids, across the stages of
217 gastrulation. We observed that the sand- *irx1b* allele was expressed at significantly higher
218 levels (average of 2.5-fold; p = 4.5e-13; Student's t-test) and that this difference was
219 largely confined to MG (Figure 2B). Next, we used hybrid embryos to chart the
220 development of the telencephalon and the eye field. Rock- x sand- F_2 hybrids, indexed
221 for *irx1b* genotype, were raised to neurula and somitogenesis stages and we examined
222 the expression of *shh* (which induces *foxg1* and the ventral forebrain), *foxg1* (a marker of
223 the telencephalon), and *rx3* (a marker of the eye field), by in situ hybridization. F_2
224 individuals homozygous for rock- *irx1b* alleles exhibited a larger and more rostral domain
225 of *shh* expression, an earlier and larger domain of *foxg1* and a smaller *rx3* domain (Figure
226 2C, D). These differences between rock- vs. sand- *irx1b* genotypes match expression
227 divergence observed amongst rock- vs. sand- species [21,22]. Finally, when we compared

the relative size of the telencephalon among *irx1b* genotypes, individuals homozygous for rock- alleles exhibited larger telencephala (Supplementary Figure 3). We conclude that genetic variants in and around the *irx1b* gene contribute to divergent specification of the Malawi cichlid forebrain, likely via spatial, temporal and quantitative variation in the expression of *irx1b* itself.

Our genome sequencing revealed a near-fixed InDel in the 3' UTR of the Malawi cichlid *irx1b* gene (Supplementary Figure 4). Rock- species possess an 85bp insertion, compared to cichlid species from outside of the Malawi lineage. Sand-dwellers largely lack the insertion and exhibit a 6bp deletion compared to outgroups. The insertion shows strong genetic similarity to a fragment from the Rex1 family of non-LTR retrotransposons [46]. Given the likelihood that *Astatotilapia calliptera* populations surrounding Lake Malawi may have seeded the Malawi evolutionary radiation and contributed to rock- and sand-dwelling lineages [17,28], we explored the presence/absence of this InDel in *Astatotilapia* samples. We found that most *Astatotilapia* individuals and populations had the rock- *irx1b* allele (the insertion), but that an individual from Chizumulu Island was fixed for the sand- allele and two individuals sampled from Itupi were heterozygous. Because the 85bp insertion in rock- species is a partial Rex1 fragment, and sand- species carry a 6bp deletion compared to outgroups, we speculate that the current rock- and sand- divergent alleles were generated by at least two imperfect excision events of an element that invaded the genome of the Malawi + *Astatotilapia* ancestor. Rex1/Babar retrotransposons have been active in African cichlid genomes, and are known to influence gene expression when inserted in 5' and 3' UTRs [31]. Future experiments will determine whether this Rex1 insertion causes the differences in *irx1b* gene expression and forebrain specification we observed.

Genomics of divergent social challenge and opportunity

Rock- and sand-dwelling Malawi cichlids live in strikingly different social and physical environments. Rock-dwelling males tend to be more aggressive than sand-dwellers [23] and defend territories year-round as sites for feeding and breeding. By contrast, sand-

dwellers are more exploratory than rock-dwellers [25] and only breeding males tend to be territorial, often building sand bowers to attract females and mitigate male-male aggression. Given these observations and genome-wide enrichment for categories related to adult behavior and social interaction, we designed an experimental paradigm to investigate brain gene expression profiles associated with divergent rock- vs. sand-social behaviors.

We evaluated social challenge and opportunity amongst males using a large tank with a 'rock' habitat at one end and 'sand' at the other, separated by glass bottom (Figure 3A). When parental rock- species are placed in this tank paradigm, males court females on the rock side of the tank. Males of sand- species court females over sand and construct species-appropriate bowers. When single hybrid rock- x sand- F_1 males are placed in this arena with hybrid F_1 females, males invariably court females over the 'rock' habitat. However, when two rock- x sand- hybrid F_1 males (brothers) were allowed to compete for gravid hybrid F_1 females in this tank paradigm, we observed something different. One male, typically the larger, courted females over the rock habitat, and the other simultaneously constructed bowers to court females over the sand. We found no difference in gonadal-somatic index (GSI), an established biological metric of reproductive status and maturity, between F_1 males behaving as 'socially rock' vs. 'socially sand.' (Supplementary Figure 5). Our observation of divergent behavior between F_1 brothers in the same tank suggests an interaction between the genome and the social environment.

We used RNA-seq to investigate gene expression profiles associated with behavior of rock- x sand- F_1 hybrid males that were actively courting females over rock vs. sand. Whole brains of F_1 males tested singly (n=2 lone) as well as F_1 brothers assayed in dyads (n=4 dyads) were collected during courtship, and interrogated by RNA-seq. Strikingly, gene expression profiles clustered not by fraternal relatedness, but rather by behavioral context (Figure 3B). Males from dyads that courted females over rocks had expression profiles similar to single males (who also courted over rocks) but distinct from their brothers that built bowers and courted females over sand in the same tank. Genes were

considered significantly differentially expressed between 'social rock' and 'social sand' brains if they exhibited both a fold change ≥ 2 and crossed the threshold of $p_{adj} < 0.05$. Based on this criterion, we found 832 genes differentially expressed between rock- vs. sand-behaving males (Figure 3B, Supplementary Table 3). Among differentially expressed genes, we observed significant functional enrichment for GO Biological Process categories 'synaptic signaling' (p < 2.3e-21), 'synaptic plasticity' (p < 3.6e-09), 'visual behavior' (p < 2.09e-06); mouse phenotypes 'abnormal learning/memory/conditioning' (p < 5.9e-07), 'abnormal telencephalon morphology' (p < 3.95e-07), 'abnormal spatial learning' (p < 9.9e-07) and pathways 'axon guidance' (p < 3.3e-05), 'oxytocin signaling' (p < 5.2e-05) and 'estrogen signaling' (p < 1.8e-04) (Supplementary Table 3). Matches against the Allen Brain Atlas database of gene expression yielded enrichment for exclusively sub-regions of the telencephalon: CA3, hippocampus (p_{adj} = 4.6e-6), CA2, hippocampus (p_{adj} = 7.3e-5), CA4, hippocampus (p_{adj} = 0.001), claustrum (p_{adj} = 0.001), subiculum (p_{adj} = 0.003), dentate gyrus (p_{adj} = 0.03) and the basomedial nucleus of the amygdala (p_{adj} = 0.03). The hippocampus encodes episodic memory and spatial representations of the environment [47], and more recently its subregions have been shown to play critical roles in anxiety, social interaction, and social memory formation [48-50]. Roughly 38% of differentially expressed genes also contained genetically differentiated SNP/InDels between rock- and sand- species (p-value < 2e-6, Fisher's exact test), implying considerable cis-acting genetic variation. Enrichment of numerous categories related to brain function and synaptic plasticity showed greater overlap than expected (Figure 3C). These context-dependent differences suggest concerted changes in brain gene expression as males experienced and responded to different social challenges and opportunities [24,51].

Discussion

A fundamental problem in evolutionary biology is understanding the cellular, developmental and genetic basis of how traits change. This is a challenge because we lack sufficient information about how genes work in outbred genomes from nature and we do not fully comprehend the causal role of noncoding variation in specifying form and function. This problem is especially difficult for traits that are only observed in particular contexts, like development and behaviour. To make progress, we and others have focused on study systems exhibiting abundant phenotypic diversity built from a relatively small number of genetic changes. Here we identify and characterize the genetic variants that demarcate one of the deepest evolutionary splits amongst Lake Malawi cichlid groups, that between rock- and sand-dwelling species thought to have diverged in the last one million years. We found a small percentage (less than 0.1%) of genetic variants to be differentiated between rock- and sand- groups, and that the majority of differentiated variants (>96%) were noncoding. Differentiated non-coding variants were more likely to be in an evolutionarily conserved locus as a function of genetic differentiation, suggesting that divergent rock- vs. sand- noncoding changes are functional. To support this idea, we identified alternately fixed rock- vs. sand- noncoding variants within experimentally verified, vertebrate-conserved craniofacial and cranial neural crest cell enhancers. The latter observation is similar in type to the discovery of human-specific deletions within mammal-conserved regulatory sequence [52].

Recently we surveyed genome-wide divergence between sand-dweller sub-groups that construct pit vs. castle bowers, sand-made structures to attract females for mating [24]. Mapping those variants to the same genome reference, we expected distinct patterns of diversification because rock-sand and pit-castle divergence likely occurred at different times, along different trait axes, under the control of different evolutionary forces [27]. Consistent with expectation, there is clear clustering of genome divergence on chromosome 11 for the pit-castle comparison (Supplementary Figure 6), while all chromosomes carry the signature of rock-sand diversification (Figure 1B). However, contrary to our expectation, rock- vs. sand- and pit- vs. castle- radiations have diverged in similar gene sets. Out of 3070 genes identified near 10kb high F_{ST} regions in the rock-

vs. sand- comparison, 483 overlap with 1090 genes identified near high F_{ST} regions in the pit- vs. castle- comparison (p-value < 2e-9, Fisher's exact test, Supplementary Table 4). This result may imply that evolutionary diversification in Lake Malawi is limited, or constrained, by chromosomal location.

Overall, genes in proximity to rock-sand divergent variants were enriched for functional categories related to early forebrain and craniofacial development, neuronal function and social behavior. This list of variants, coupled with consistent patterns of functional and pathway enrichment, motivated follow up experiments focused on early brain development and adult social behavior (Figure 4). It is apparent from our work here and previously [21,22], that Malawi cichlid brains and nervous systems begin to differ during gastrulation in pathways that can be predicted from divergent genome sequences. This is interesting for at least two reasons. First, this observation runs counter to the 'late equals large' textbook example [53] of how brains evolve differences in relative proportions of their parts [22]. Similarly, such early variation in development is not thought to be a driving force in evolution, precisely because early changes can have global and ramifying effects. Collectively, our findings provide a partial description of the conditions wherein variation during the earliest stages of development can contribute to evolutionary diversification. In each case we have examined, variation in gene expression is quantitative, heterochronic and limited to a precise stage or time period.

Sydney Brenner recognized the relationship between the genetic specification of nervous systems and the behavioral output of the brain [54]. However, because these events take place so far apart in the lifespan of a vertebrate, they are rarely studied simultaneously. Here, the genome connects the two phenomena: rock- vs. sand- divergent gene sets indicating that both brain development and social behavior have been under divergent selection during the evolutionary diversification of these groups. To evaluate social behavior in rock- vs. sand-dwelling Malawi cichlids, we constructed a social context arena. The presence of sand and simulated rocky caves was sufficient to elicit species-appropriate male behavior when rock- or sand- males were tested with rock- or sand-gravid females. When rock- x sand- F_1 hybrid males were tested, one per tank, with F_1

hybrid females, males courted females in the rock quadrant of the tank. Notably, when dyads of F_1 brothers were tested in this tank paradigm with gravid F_1 females, we observed simultaneous 'social rock' and 'social sand' behavior. Brain gene expression profiles from behaving males clustered by social context (social rock vs social sand), and not by fraternal relationships. Differentially expressed genes were enriched for brain regions and pathways implicated in social interaction and overlapped significantly with rock- vs. sand- divergent genetic variants.

Social context is known to influence the brain. For instance, our clustering results are similar to those of Whitfield and colleagues (Whitfield et al. 2003) who showed that brain gene expression in honey bees was predictive of behavior. Likewise, changes in brain morphology and gene expression predictably accompany the ascent to dominance in the cichlid fish *Astatotilapia burtoni* [55]. Our data seem not to fit the model of dominant-subordinate however. In our experiments, the gonado-somatic index (GSI) did not differ between social rock vs. social sand brothers within dyads. Both males exhibited nuptial coloration, courted females and in cases with multiple gravid females, both brothers reproduced. Body size was associated with divergent social rock vs. social sand behavior of F_1 males; the social rock brother was always larger (mean mass was 26.96g ± 3.4 [SE] compared to 19.45g ± 2.2).

Our experiments demonstrate that F_1 hybrid male brains can express both social rock- and social sand- behavioral programs, and that social context determines which program is executed. This observation is similar to, but also different than, pit-digging x castle-building F_1 male Malawi cichlids who carry out parental bower behaviors in a specific sequence [24]. Notably, in both cases, the hybrid males exhibit one of the two different parental behaviors at any one time – there is no intermediate behavior. In the pit- vs. castle- case, we think that the bower structure itself and/or a threshold signal from females might lock the hybrid male brain into a behavioral state. In the rock- vs sand- case here, it appears that other social cues (i.e., the presence and size of a rival male) lock the hybrid male brain into a behavioral state. These context-dependent behaviors, accompanied by changes in brain gene expression, are compelling examples of interaction between the

genome and the social environment. The cellular and genetic basis of these behaviors and their plasticity deserves further attention. Our comparative genomic and brain gene expression data, combined with enrichment testing and experimental approaches, highlight that the Malawi cichlid telencephalon will be central to this future work.

Materials and Methods

Genome sequencing

We extracted genomic DNA, from fin clips of 22 male individuals (Qiagen DNeasy, Cat #69504), from 8 rock dwelling and 14 sand dwelling Lake Malawi species (Supplementary Table 2) representing broad diversity across the rock and sand lineages in Lake Malawi. We made libraries using the Illumina Nextera Library prep kit and performed paired-end sequencing on the Illumina Hi-Seq 2500 at Georgia Tech. The *Metriaclima zebra* reference genome version MZ_UMD2a [30] was used for genome alignment, variant discovery and annotation using standard BWA [56] and GATK practices [57]. The maximum likelihood tree in Figure 1A was constructed using SNPhylo [58], from variant data.

Genetically Divergent Regions

Vcftools [59] was used to calculate F_{ST} (--weir-fst-pop) between the 8 rock and 14 sand species. Variants with $F_{ST} = 1$ were noted to be alternately fixed between rock and sand lineages in our dataset. F_{ST} was also measured across 10kb windows (--fst-window-size). Significance thresholds were marked using the fdrtool package in R. All variants were annotated using Snpeff 4.3i [60]. We tested the genes within 25 kb of significantly differentiated variants for enrichment of functional categories. The cichlid gene names were converted to human analogs using Treefam based mapping [61] and functional enrichment was determined using the TOPPFUN web-browser interface [62].

PhastCons analysis

Pairwise alignments were generated using lastz v1.02[63], with the following parameters: "B=2 C=0 E=150 H=0 K=4500 L=3000 M=254 O=600 Q=human_chimp.v2.q T=2 Y=15000". This was followed by using USCS genome utilities (https://genome.ucsc.edu/util.html, https://hgdownload.soe.ucsc.edu/admin/exe/linux.x86_64/FOOTER) axtChain tool with -minScore=5000. Additional tools with default parameters were then used following the

UCSC whole-genome alignment paradigm (http://genomewiki.ucsc.edu/index.php/Whole_genome_alignment_howto) in order to obtain a contiguous pairwise alignment. Multiple alignments were generated from pairwise alignments with the multiz v11.2 [64] program, using default parameters and the following pre-determined phylogenetic tree: ((((*M. zebra*, *P. nyererei*), *A. burtoni*), *N. brichardi*), *O. niloticus*) in agreement with Brawand et al. [31]. Sequence conservation scores were then obtained using PhastCons [65] with a phylogenetic model estimated by the phyloFit [66] program, both from the PHAST software package (v.1.3). The model fitting was done using default parameters. PhastCons was run in two iterations, first to obtain the free parameters of the model (--estimate-trees and --no-post-probs) and then using the output from this we ran PhastCons again to attain the conservation scores with --target-coverage 0.3 --expected-length 100.

Vertebrate-conserved enhancer elements

A comparative genomic approach was used to identify putative craniofacial and neural crest CNEs in mammals that segregate SNPs between rock-sand cichlid species. Experimentally verified and published genome-wide craniofacial and neural crest enhancers active during early embryonic stages that play a role in shaping the development of neural crest and craniofacial structures in mammals were identified from published literature [39,40]. We used the liftOver tool [67], which maps orthologous genomic regions between species to convert genomic coordinates from one species to another. Using a Human to *Oreochromis niloticus* to *Metriaclima zebra* mapping and a Mouse to *Oreochromis niloticus* to *Metriaclima zebra* mapping, we identified the orthologous genomic locations of the published craniofacial and neural crest enhancers in cichlids. We designated any alternately fixed variant (variant with $F_{ST} = 1$) that was also within an orthologous CNE as putatively involved in the rock-sand divergence (Supplementary Table 2).

Brain region enrichment analysis

We identified 10,391 cichlid genes with human homologues and generated an expression matrix for each gene across 250 human brain structures spanning telencephalon, diencephalon, mesencephalon, and metencephalon using adult human brain microarray data collected by the Allen Brain Institute [33]. Cortical regions and gyri for which fish do not have putative homologues were excluded from the analysis (100/350, leaving 250 regions for subsequent analysis). The expression matrix was generated using the get_expression function in the ABAEnrichment Bioconductor package in R [68]. We then calculated the specificity of expression for each gene in each of these brain regions using the specificity.index function in the pSI package for R. This function calculates a matrix of gene expression specificity indices, and corresponding p-values, as described previously [69,70]. We then tested whether 1) genes within 25kb of rock vs. sand significantly differentiated variants (described above under "Genetically Divergent Regions"), and 2) genes that were differentially expressed between rock- vs. sand-behaving F1 hybrid males, were enriched for transcriptional markers of specific brain regions using the *fisher.iteration* function with Benjamini-Hochberg correction, again using the pSI package for R. For enrichment testing of differentially expressed genes, we restricted analysis to genes that met the following criteria: 1) transcripts for the gene were detected in all eight paired behaving males, and 2) at least 6 transcripts were detected in each subject.

Staging during gastrulation

Cichlid gastrulation was split into three sub stages within the gastrula stage 9 [71]. Gastrulation lasts 8 to 12 hours, depending on the species, and is defined as after the shield (as described in zebrafish) stage until the presence of the first somite at the beginning of neurula (stage 10). Embryos were classified as early gastrula (EG) by an asymmetry in epiboly after shield stage until the formation of a ridge that is analogous to the anterior neural ridge (ANR) in chick and mouse and the anterior neural border (ANB) in zebrafish. At that point embryos were classified as mid gastrula (MG). MG lasts until the formation of the dorsal-ventral axis, defined by further lengthening of one side of the embryo, which begins to thicken as epiboly progresses. This is the dorsal side of the embryo, and the side opposite the ANR is classified the ventral side of the embryo. At this

point the embryos are defined as late gastrula (LG). LG ends with the specification of the neural plate, which appears as a portion of the dorsal embryo that is raised relative to ventral side, usually in line with the ANR.

Immunohistochemical staining

Embryos were harvested at 24 hours post fertilization (hpf) from each of the rock -dwelling cichlids *Metriaclima patricki* and *Metriaclima zebra* and the sand-dwelling cichlid *Copadichromis borleyi* and *Tramitichromis intermedius*. The embryos were cultured until they reached gastrula stage, approximately 36 to 40 hpf, then fixed at intervals throughout gastrula until neurula. The embryos were then treated with auto-fluorescence reducer (1.55mL 5M NaCl, 250ul Tris-HCl, pH 7.5, and 95mg NaBH4) overnight, and 10% 2-mercaptoethanol for 1 hour. Next, whole mount *in situ* hybridization was done, using a modification methods we published previously [72]. *irx1b* was visualized using Fast Red (naphthol chromogen, Roche Diagnostics), which fluoresces at near red wavelengths (500-650 nm). After *in situ* hybridization, embryos were immunostained for pSMAD 1,5,8 protein, using published protocols [73]. Embryos were then bathed in Vectashield (Vector Labs) containing DAPI and placed in a specially built mold[45] that accommodates the large yolk and holds the embryo upright. Embryos were then scanned using a Zeiss LSM 700-405 confocal microscope and processed using LSM 700 software and Image J.

Rock-Sand hybridization and genotyping

Two rock-sand crosses, one between *Copadichromis borleyi* (CB, sand-dweller sire) and *Metriaclima zebra* (MZ, rock-dweller dam) and another between *Mchenga conophoros* (MC, sand- sire) and *Petrotilapia sp.* 'thick bar' (PT, rock- dam), were artificially generated by taking the eggs from the dam just prior to spawning and mixing with sperm from the sire. The resultant F_1 were grown in tanks and allowed to spawn normally to generate F_2. Several F_2 broods were taken from multiple F_1 females for each cross, a total of 355 individuals for the CB x MZ cross and 608 for the MC x PT cross. The embryos were fixed at every stage starting at gastrula (stage 9) until early pharyngula (stage 14). The F_2

embryos were RNA-extracted at stage 9. DNA extraction was performed by fixing the embryos (stage 11-14) in 70% ethanol, then removing the tail from each individual and extracting the DNA using an extraction kit (Qiagen). Following extraction, the F_2 embryos were genotyped using custom probes (CAAATCTCCC[C/T]CCGCGGC, Taqman custom probes, Invitrogen) designed to identify a SNP in *irx1b* using RT-PCR. A subset of the embryos was also sequenced at a 900 bp interval around the *irx1b* SNP to verify the custom probes.

Quantitative F_2 Analysis

We quantified *irx1b* in F_2 at stage 9 and separated by genotypic class. The 74 heterozygous rock X sand F_2 embryos were dissected to remove most of the yolk and the total RNA was extracted from each individual using an RNA Extraction Kit (Qiagen). The amount of mRNA specific to each allele of *irx1b* was quantified by using the RNA-to-Ct kit (Invitrogen) and the custom probes. The delta Ct for each heterozygote was generated with the equation, 2^(allele from dam – allele from sire). We tested the data with an ANOVA, followed by a Tukey's multiple comparison test to determine significance between genotype classes.

Forebrain and eye measurements

The forebrain and eyes were measured by integrating the area of transverse sections in embryos of rock- and sand-dweller cichlid species, using previously published methods [21]. The rock-dweller species included *Cynotilapia afra* (CA, planktivore), *Labeotropheus fuelleborni* (LF, algivore) and *Metriaclima zebra* (MZ, generalist); sand-dweller species included *Aulonocara jacobfreibergi* (AJ, 'sonar' hunter), *Copadichromis borleyi* (CB, planktivore) and *Mchenga conophoros* (MC, insectivore/generalist). Embryos from each species, as well as the F_2 individuals, were measured starting from the earliest the telencephalon can be differentiated from the forebrain (mid-somitogenesis, stage 12) and at each subsequent stage until the forebrain has defined prosomeres (early pharyngula, stage 14) [22]. To keep measurements standardized across stages, all measurements were

555 defined by forebrain morphology at the earliest timepoint (stage 12). The 'eye'
556 measurement remains consistent at all stages, the 'anterior' measurement includes the
557 telencephalon and presumptive olfactory bulb, and the 'posterior' measurement includes
558 the diencephalon and each of its constitutive prosomeres (dorsal and ventral thalamus
559 and hypothalamus). To facilitate measurements, we used gene expression of *rx3* (for
560 stage 12 embryos) and *pax6* (stage 13 and 14) to identify the different structures of the
561 forebrain and eye.
562

563 *RNA Extraction and Sequencing, Adult Social Behavior*

564

565 Two adult F_1 hybrid males from rock- x sand- interspecific crosses (Supplementary table
566 5) were introduced to an assay tank containing 3-5 hybrid females of the same cross with
567 simulated rock habitat on one side and simulated sand habitat on the other side separated
568 by empty tank space (Figure 3A). Males were observed over a period of four days for
569 courtship behavior, either similar to a rock parent (courting females over the rocky parts
570 of the tank), here designated "social rock" --- or to a sand parent (bower building in the
571 sand side of the tank while courting females), here designated "social sand." When
572 courtship behavior of both males was observed, we primed experiments the next morning
573 by resetting the tanks -- knocking down or filling in the sand bower, and adjusting the rock
574 habitat. Both males were allowed to exhibit courtship behavior over a period of 90
575 minutes. Males were sacrificed immediately after this 90-minute period by rapid
576 decapitation and whole brains were immediately stored in RNAlater (Thermo Fisher Cat#
577 AM7020) within 20 minutes of decapitation. Two tanks with one F_1 male and 3-5 F_1
578 females were also observed. These males exhibited social rock behavior and were
579 designated as "lone" in the behavior assay; their brains were collected in the exact same
580 way as the other samples.
581

582 Tissues were frozen in liquid nitrogen, homogenized using a mortar and pestle and placed
583 in trizol. Following standard chloroform extraction, RNeasy mini columns (Qiagen Cat
584 No./ID: 74104) were utilized to purify RNA for sequencing. Total RNA was quantified

using Qubit (Molecular Probes) and quality analyzed using the Agilent 2100 Bioanalyzer System for RNA library preparation. RNA input was normalized to 1µg and libraries were prepared using the TruSeq Stranded mRNA Sample Prep Kit (Illumina- Kit A). Libraries were again quantified, quality assessed, and normalized for sequencing on the HiSeq 2500 Illumina Sequencing System (Georgia Tech Genomics Core, standard practices). Experimental design and raw files can be accessed on the NCBI Gene Expression Omnibus database under the accession number GSE122500.

Differential Gene Expression Analysis

Raw sequence reads from whole brain transcriptomes were quality controlled using the NGS QC Toolkit [74]. Raw reads with an average PHRED quality score below 20 were filtered out. Filtered reads were also trimmed of low-quality bases at the 3' end. High quality sequence reads were aligned to the *M.zebra* reference genome MZ_UMD2a[30] using TopHat v2.0.9 [75]. On average, across all samples, over 95% of reads mapped to the reference genome. The resulting TopHat2 output bam files were sorted and converted to sam files using samtools v0.19 [76]. Sorted sam files were used as input for the HTSeq-count v0.6.1 program to obtain fragment counts for each locus [77]. Fragment counts were scale-normalized across all samples using the calcNormFactors function in the edgeR package v3.6.8 [78]. Relative consistency among replicates and samples was determined via the Multidimensional scaling (MDS) feature within the edgeR package in R. The native R function *hclust(dist)* used to cluster samples. Scale-normalized fragment counts were converted into $\log_2$ counts per million reads mapped (cpm) with precision weights using voom and fit to a linear model using limma v3.20.9 [79]. Pairwise contrasts were constructed between socially rock and socially sand samples. After correcting for multiple comparisons using the Benjamini-Hochberg method [80], genes were considered differentially expressed between socially rock and socially sand samples if they exhibited both a fold change ≥ 2 and $P_{adj} < 0.05$. Using Treefam based mapping [61] the cichlid gene names were converted to human analogs and functional enrichment was determined using the TOPPFUN web-browser [62].

614 *Ethics Statement*

615 All of the animals were handled according to methods approved by the Georgia Tech
616 Institutional Animal Care and Use Committee (IACUC) protocols (permit A100029) with
617 every effort made to minimize suffering and is in compliance with the ARRIVE guidelines.

Acknowledgements: This work was supported by grants from the NIH (R01GM101095, 2R01DE019637-10 to JTS and F32GM128346-01A1 to ZVJ) and the Human Frontiers Science Program (RGP0052/2019 to JTS). We would like to thank Shweta Biliya and the Genomics Core at Georgia Tech for invaluable assistance with the NGS sequencing. We also thank the members of the Streelman lab for comments on this manuscript.

References

1 Boyle, E. A., Li, Y. I. & Pritchard, J. K. An Expanded View of Complex Traits: From Polygenic to Omnigenic. *Cell* **169**, 1177-1186, doi:10.1016/j.cell.2017.05.038 (2017).

2 Fields, C., Adams, M. D., White, O. & Venter, J. C. How many genes in the human genome? *Nature Genetics* **7**, 345-346, doi:10.1038/ng0794-345 (1994).

3 Maurano, M. T. *et al.* Systematic localization of common disease-associated variation in regulatory DNA. *Science*, 9718-9723 (2012).

4 Degner, J. F. *et al.* DNase I sensitivity QTLs are a major determinant of human expression variation. *Nature* **482**, 390 (2012).

5 Streelman, J., Peichel, C. L. & Parichy, D. Developmental genetics of adaptation in fishes: the case for novelty. *Annu. Rev. Ecol. Evol. Syst.* **38**, 655-681 (2007).

6 Colosimo, P. F. *et al.* The genetic architecture of parallel armor plate reduction in threespine sticklebacks. *Plos Biol* **2**, E109, doi:10.1371/journal.pbio.0020109 (2004).

7 Kratochwil, C. F. *et al.* Agouti-related peptide 2 facilitates convergent evolution of stripe patterns across cichlid fish radiations. *Science* **362**, 457-460, doi:10.1126/science.aao6809 (2018).

8 Albertson, R. C., Streelman, J. T., Kocher, T. D. & Yelick, P. C. Integration and evolution of the cichlid mandible: The molecular basis of alternate feeding strategies. *P Natl Acad Sci USA* **102**, 16287-16292, doi:DOI 10.1073/pnas.0506649102 (2005).

9 Shapiro, M. D. *et al.* Genomic diversity and evolution of the head crest in the rock pigeon. *Science* **339**, 1063-1067, doi:10.1126/science.1230422 (2013).

10 Lamichhaney, S. *et al.* Evolution of Darwin's finches and their beaks revealed by genome sequencing. *Nature* **518**, 371-375 (2015).

11 Okhovat, M., Berrio, A., Wallace, G., Ophir, A. G. & Phelps, S. M. Sexual fidelity trade-offs promote regulatory variation in the prairie vole brain. *Science* **350**, 1371-1374 (2015).

12 Bendesky, A. *et al.* The genetic basis of parental care evolution in monogamous mice. *Nature* **544**, 434 (2017).

13 Pfenning, A. R. *et al.* Convergent transcriptional specializations in the brains of humans and song-learning birds. *Science* **346**, 1256846 (2014).

14 Greenwood, A. K., Wark, A. R., Yoshida, K. & Peichel, C. L. Genetic and neural modularity underlie the evolution of schooling behavior in threespine sticklebacks. *Curr Biol* **23**, 1884-1888, doi:10.1016/j.cub.2013.07.058 (2013).

15 Kocher, T. D. Adaptive evolution and explosive speciation: The cichlid fish model. *Nat Rev Genet* **5**, 288-298 (2004).

16 Loh, Y. H. E. *et al.* Comparative analysis reveals signatures of differentiation amid genomic polymorphism in Lake Malawi cichlids. *Genome Biology* **9** (2008).

17 Loh, Y. H. E. *et al.* Origins of Shared Genetic Variation in African Cichlids. *Mol Biol Evol* **30**, 906-917 (2013).

18 Streelman, J. T., Albertson, R. C. & Kocher, T. D. Genome mapping of the orange blotch colour pattern in cichlid fishes. *Mol Ecol* **12**, 2465-2471, doi:10.1046/j.1365-294x.2003.01920.x (2003).

19 Roberts, R. B., Ser, J. R. & Kocher, T. D. Sexual conflict resolved by invasion of a novel sex determiner in Lake Malawi cichlid fishes. *Science* **326**, 998-1001 (2009).

20 Parnell, N. F. & Streelman, J. T. Genetic interactions controlling sex and color establish the potential for sexual conflict in Lake Malawi cichlid fishes. *Heredity* **110**, 239-246 (2013).

21 Sylvester, J. B. *et al.* Competing signals drive telencephalon diversity. *Nat Commun* **4**, 4 (2013).

22 Sylvester, J. B. *et al.* Brain diversity evolves via differences in patterning. *Proceedings of the National Academy of Sciences* **107**, 9718-9723 (2010).

23 Baran, N. M. & Streelman, J. T. Ecotype differences in aggression, neural activity and behaviorally relevant gene expression in cichlid fish. *Genes Brain Behav* **19**, e12657, doi:10.1111/gbb.12657 (2020).

24 York, R. A. *et al.* Behavior-dependent cis regulation reveals genes and pathways associated with bower building in cichlid fishes. *Proceedings of the National Academy of Sciences* **115**, E11081-e11090, doi:10.1073/pnas.1810140115 (2018).

25 Johnson, Z. V. *et al.* Exploratory behaviour is associated with microhabitat and evolutionary radiation in Lake Malawi cichlids. *Animal Behaviour* **160**, 121-134, doi:https://doi.org/10.1016/j.anbehav.2019.11.006 (2020).

26 Fraser, G. J. *et al.* An ancient gene network is co-opted for teeth on old and new jaws. *Plos Biol* **7**, e1000031 (2009).

27 Streelman, J. T. & Danley, P. D. The stages of vertebrate evolutionary radiation. *Trends Ecol Evol* **18**, 126-131 (2003).

28 Malinsky, M. *et al.* Whole-genome sequences of Malawi cichlids reveal multiple radiations interconnected by gene flow. *Nat Ecol Evol* **2**, 1940-1955, doi:10.1038/s41559-018-0717-x (2018).

29 McKaye, K. R., Louda, S. M. & Jay R. Stauffer, J. Bower Size and Male Reproductive Success in a Cichlid Fish Lek. *The American Naturalist* **135**, 597-613, doi:10.1086/285064 (1990).

30 Conte, M. A. *et al.* Chromosome-scale assemblies reveal the structural evolution of African cichlid genomes. *GigaScience* **8**, doi:10.1093/gigascience/giz030 (2019).

31 Brawand, D. *et al.* The genomic substrate for adaptive radiation in African cichlid fish. *Nature* **513**, 375-381 (2014).

32 Ben-Ari Fuchs, S. *et al.* GeneAnalytics: An Integrative Gene Set Analysis Tool for Next Generation Sequencing, RNAseq and Microarray Data. *Omics* **20**, 139-151 (2016).

33 Hawrylycz, M. J. *et al.* An anatomically comprehensive atlas of the adult human brain transcriptome. *Nature* **489**, 391-399, doi:10.1038/nature11405 (2012).

34 Adhikari, A. *et al.* Basomedial amygdala mediates top-down control of anxiety and fear. *Nature* **527**, 179-185, doi:10.1038/nature15698 (2015).

35 Mesquita, L. T. *et al.* New insights on amygdala: Basomedial amygdala regulates the physiological response to social novelty. *Neuroscience* **330**, 181-190, doi:https://doi.org/10.1016/j.neuroscience.2016.05.053 (2016).

36 Carvalho, F. R., Nóbrega, C. D. R. & Martins, A. T. Mapping gene expression in social anxiety reveals the main brain structures involved in this disorder. *Behavioural Brain Research* **394**, 112808, doi:https://doi.org/10.1016/j.bbr.2020.112808 (2020).

37 Abrahams, B. S. *et al.* SFARI Gene 2.0: a community-driven knowledgebase for the autism spectrum disorders (ASDs). *Mol Autism* **4**, 36, doi:10.1186/2040-2392-4-36 (2013).

38 Piñero, J. *et al.* DisGeNET: a comprehensive platform integrating information on human disease-associated genes and variants. *Nucleic Acids Research* **45**, D833-D839, doi:10.1093/nar/gkw943 (2017).

39 Attanasio, C. *et al.* Fine Tuning of Craniofacial Morphology by Distant-Acting Enhancers. *Science* **342** (2013).

40 Rada-Iglesias, A. *et al.* Epigenomic Annotation of Enhancers Predicts Transcriptional Regulators of Human Neural Crest. *Cell Stem Cell* **11**, 633-648 (2012).

41 Simoes-Costa, M. & Bronner, M. E. Establishing neural crest identity: a gene regulatory recipe. *Development* **142**, 242-257, doi:10.1242/dev.105445 (2015).

42 Roberts, R. B., Hu, Y., Albertson, R. C. & Kocher, T. D. Craniofacial divergence and ongoing adaptation via the hedgehog pathway. *Proc Natl Acad Sci U S A* **108**, 13194-13199, doi:10.1073/pnas.1018456108 (2011).

43 Cavodeassi, F., Modolell, J. & Gómez-Skarmeta, J. L. The Iroquois family of genes: from body building to neural patterning. *Development* **128**, 2847-2855 (2001).

44 Bielen, H. & Houart, C. BMP signaling protects telencephalic fate by repressing eye identity and its Cxcr4-dependent morphogenesis. *Developmental cell* **23**, 812-822 (2012).

45 White, D. E. *et al.* Quantitative multivariate analysis of dynamic multicellular morphogenic trajectories. *Integrative Biology* **7**, 825-833, doi:10.1039/c5ib00072f (2015).

46 Volff, J. N., Korting, C. & Schartl, M. Multiple lineages of the non-LTR retrotransposon Rex1 with varying success in invading fish genomes. *Mol Biol Evol* **17**, 1673-1684, doi:10.1093/oxfordjournals.molbev.a026266 (2000).

47 Olton, D. S., Becker, J. T. & Handelmann, G. E. Hippocampus, space, and memory. *Behavioral and Brain sciences* **2**, 313-322 (1979).

48 Hitti, F. L. & Siegelbaum, S. A. The hippocampal CA2 region is essential for social memory. *Nature* **508**, 88-92 (2014).

49 Chiang, M.-C., Huang, A. J., Wintzer, M. E., Ohshima, T. & McHugh, T. J. A role for CA3 in social recognition memory. *Behavioural brain research* **354**, 22-30 (2018).

50 Zou, D. *et al.* DREADD in parvalbumin interneurons of the dentate gyrus modulates anxiety, social interaction and memory extinction. *Current Molecular Medicine* **16**, 91-102 (2016).

51 O'Connell, L. A. & Hofmann, H. A. Evolution of a vertebrate social decision-making network. *Science* **336**, 1154-1157 (2012).

52 McLean, C. Y. *et al.* Human-specific loss of regulatory DNA and the evolution of human-specific traits. *Nature* **471**, 216-219, doi:10.1038/nature09774 (2011).

53 Finlay, B. L. & Darlington, R. B. Linked regularities in the development and evolution of mammalian brains. *Science* **268**, 1578-1584, doi:10.1126/science.7777856 (1995).

54 Brenner, S. Genetics of Caenorhabditis-Elegans. *Genetics* **77**, 71-94 (1974).

55 Fernald, R. D. & Maruska, K. P. Social information changes the brain. *Proc Natl Acad Sci U S A* **109 Suppl 2**, 17194-17199, doi:10.1073/pnas.1202552109 (2012).

56 Li, H. & Durbin, R. Fast and accurate short read alignment with Burrows-Wheeler transform. *Bioinformatics* **25**, 1754-1760, doi:10.1093/bioinformatics/btp324 (2009).

57 Van der Auwera, G. A. *et al.* From FastQ data to high confidence variant calls: the Genome Analysis Toolkit best practices pipeline. *Current protocols in bioinformatics* **43**, 11.10.11-33, doi:10.1002/0471250953.bi1110s43 (2013).

58 Lee, T. H., Guo, H., Wang, X. Y., Kim, C. & Paterson, A. H. SNPhylo: a pipeline to construct a phylogenetic tree from huge SNP data. *Bmc Genomics* **15** (2014).

59 Danecek, P. *et al.* The variant call format and VCFtools. *Bioinformatics* **27**, 2156-2158 (2011).

60 Cingolani, P. *et al.* A program for annotating and predicting the effects of single nucleotide polymorphisms, SnpEff: SNPs in the genome of Drosophila melanogaster strain w(1118); iso-2; iso-3. *Fly* **6**, 80-92 (2012).

61 Ramakrishnan Varadarajan, A., Mopuri, R., Streelman, J. T. & McGrath, P. T. Genome-wide protein phylogenies for four African cichlid species. *BMC Evol Biol* **18**, 1, doi:10.1186/s12862-017-1072-2 (2018).

62 Chen, J., Bardes, E. E., Aronow, B. J. & Jegga, A. G. ToppGene Suite for gene list enrichment analysis and candidate gene prioritization. *Nucleic Acids Res* **37**, W305-W311, doi:10.1093/nar/gkp427 (2009).

63 Harris, R. S. *Improved Pairwise Alignment of Genomic DNA* Doctor of Philosophy thesis, The Pennsylvania State University, (2007).

64 Blanchette, M. *et al.* Aligning multiple genomic sequences with the threaded blockset aligner. *Genome research* **14**, 708-715 (2004).

65 Siepel, A. *et al.* Evolutionarily conserved elements in vertebrate, insect, worm, and yeast genomes. *Genome Res* **15**, 1034-1050, doi:10.1101/gr.3715005 (2005).

66 Siepel, A. & Haussler, D. Phylogenetic estimation of context-dependent substitution rates by maximum likelihood. *Mol Biol Evol* **21**, 468-488 (2004).

67 Kent, W. J. *et al.* The human genome browser at UCSC. *Genome research* **12**, 996-1006 (2002).

68 Grote, S., Prufer, K., Kelso, J. & Dannemann, M. ABAEnrichment: an R package to test for gene set expression enrichment in the adult and developing human brain. *Bioinformatics* **32**, 3201-3203, doi:10.1093/bioinformatics/btw392 (2016).

69 Dougherty, J. D., Schmidt, E. F., Nakajima, M. & Heintz, N. Analytical approaches to RNA profiling data for the identification of genes enriched in specific cells. *Nucleic Acids Res* **38**, 4218-4230, doi:10.1093/nar/gkq130 (2010).

70 Xu, X., Wells, A. B., O'Brien, D. R., Nehorai, A. & Dougherty, J. D. Cell type-specific expression analysis to identify putative cellular mechanisms for neurogenetic disorders. *J Neurosci* **34**, 1420-1431, doi:10.1523/JNEUROSCI.4488-13.2014 (2014).

71 Murata, Y. *et al.* Allometric growth of the trunk leads to the rostral shift of the pelvic fin in teleost fishes. *Dev Biol* **347**, 236-245, doi:10.1016/j.ydbio.2010.07.034 (2010).

72 Fraser, G. J., Bloomquist, R. F. & Streelman, J. T. A periodic pattern generator for dental diversity. *Bmc Biol* **6** (2008).

73 Tucker, J. A., Mintzer, K. A. & Mullins, M. C. The BMP signaling gradient patterns dorsoventral tissues in a temporally progressive manner along the anteroposterior axis. *Dev Cell* **14**, 108-119, doi:10.1016/j.devcel.2007.11.004 (2008).

74 Patel, R. K. & Jain, M. NGS QC Toolkit: A Toolkit for Quality Control of Next Generation Sequencing Data. *PLoS One* **7**, 7 (2012).

75 Trapnell, C., Pachter, L. & Salzberg, S. L. TopHat: discovering splice junctions with RNA-Seq. *Bioinformatics* **25**, 1105-1111 (2009).

76 Li, H. *et al.* The Sequence Alignment/Map format and SAMtools. *Bioinformatics* **25**, 2078-2079 (2009).

77 Anders, S., Pyl, P. T. & Huber, W. HTSeq--a Python framework to work with high-throughput sequencing data. *Bioinformatics* **31**, 166-169 (2015).

78 Robinson, M. D., McCarthy, D. J. & Smyth, G. K. edgeR: a Bioconductor package for differential expression analysis of digital gene expression data. *Bioinformatics* **26**, 139-140 (2010).

79 Ritchie, M. E. *et al.* limma powers differential expression analyses for RNA-sequencing and microarray studies. *Nucleic Acids Res* **43**, e47 (2015).

80 Hochberg, Y. & Benjamini, Y. More powerful procedures for multiple significance testing. *Stat Med* **9**, 811-818 (1990).

81 Bloomquist, R. F., Fowler, T. E., Sylvester, J. B., Miro, R. J. & Streelman, J. T. A compendium of developmental gene expression in Lake Malawi cichlid fishes. *BMC Dev Biol* **17**, 3, doi:10.1186/s12861-017-0146-0 (2017).

82 Bonkowsky, J. L. *et al.* Domain-specific regulation of foxP2 CNS expression by lef1. *BMC Dev Biol* **8**, 103, doi:10.1186/1471-213X-8-103 (2008).

83 Shi, Z. *et al.* miR-9 and miR-140-5p target FoxP2 and are regulated as a function of the social context of singing behavior in zebra finches. *J Neurosci* **33**, 16510-16521, doi:10.1523/JNEUROSCI.0838-13.2013 (2013).

Author Contributions: CP, JBS, KA and JTS designed research; CP, JBS, KA, MWN, KP, RFB performed research; CP, KA, MM, ZVJ and PTM analyzed data; CP, JBS, ZVJ and JTS wrote the paper.

Competing Interest Statement: The Authors declare no competing interests.

Figures:

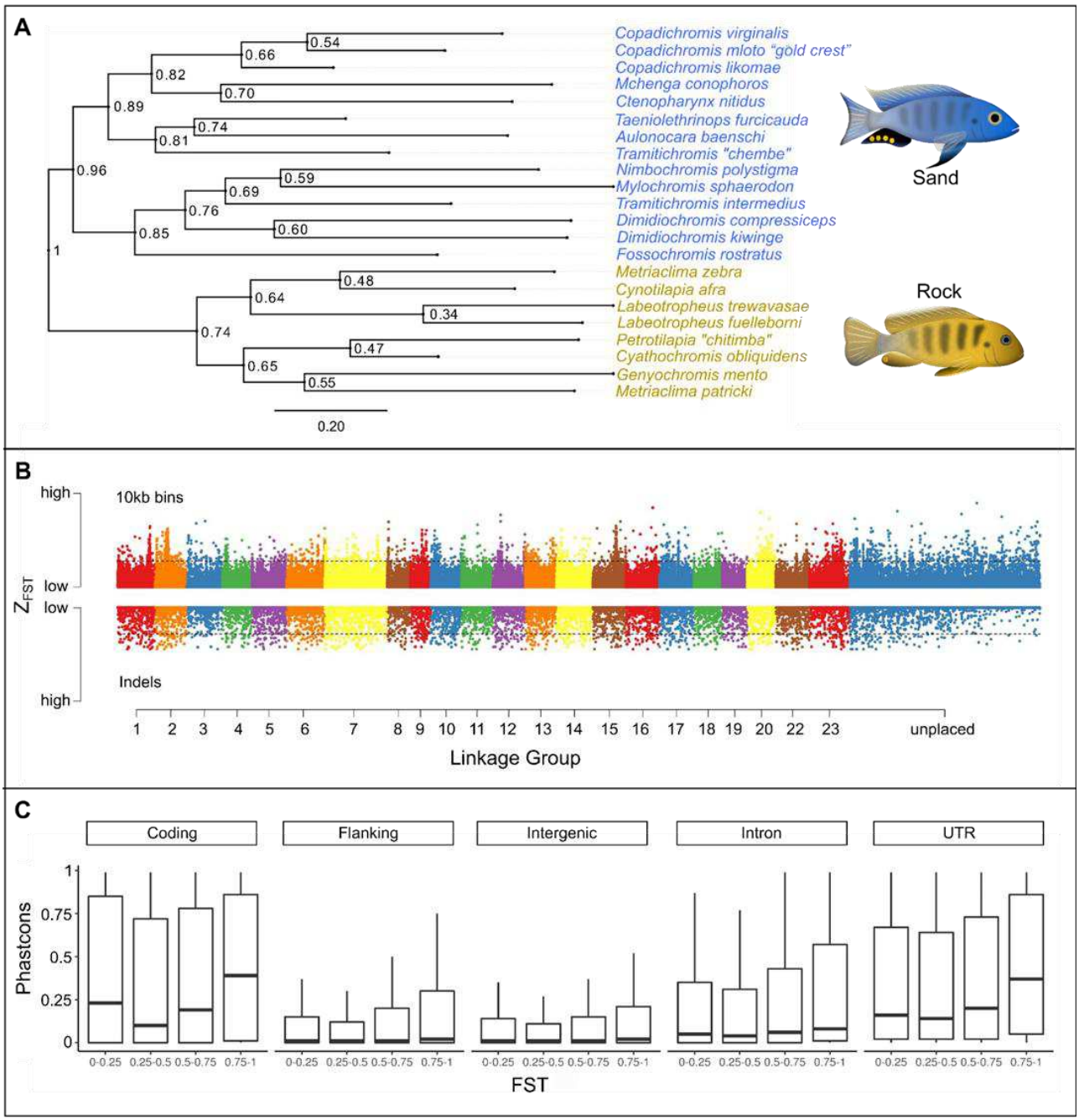

Figure 1: The genomic substrate for rock vs. sand evolution | (A) A maximum likelihood phylogeny of eight rock- and fourteen sand-dwelling species, based on variable sites (informative SNP and InDels) identified throughout the genome. “Sand” species contain representatives of the lineages “shallow benthic, deep benthic and utaka” from [28], while the “rock” species correspond to the “mbuna” lineage. (B) A plot of Z-F_{ST} (F_{ST} normalized using Fisher’s Z-transformation) across the genome, plotting genomic divergence

between rock- vs. sand-dwelling groups. Single nucleotide polymorphisms (SNPs) summed over 10kb bins and insertion-deletion mutations (InDels) are shown on the same scale. Numbers along the x-axis refer to linkage groups (i.e., chromosomes) and threshold lines indicate 2.5% FDR. (C) Evolutionary conservation (PhastCons) scores were calculated for each nucleotide across the genome, subdivided by genome annotation and plotted by bins of increasing F_{ST}. The PhastCons score for each genome category is significantly higher for increasing bins of F_{ST} (Wilcoxon rank sum p value < 2e-16).

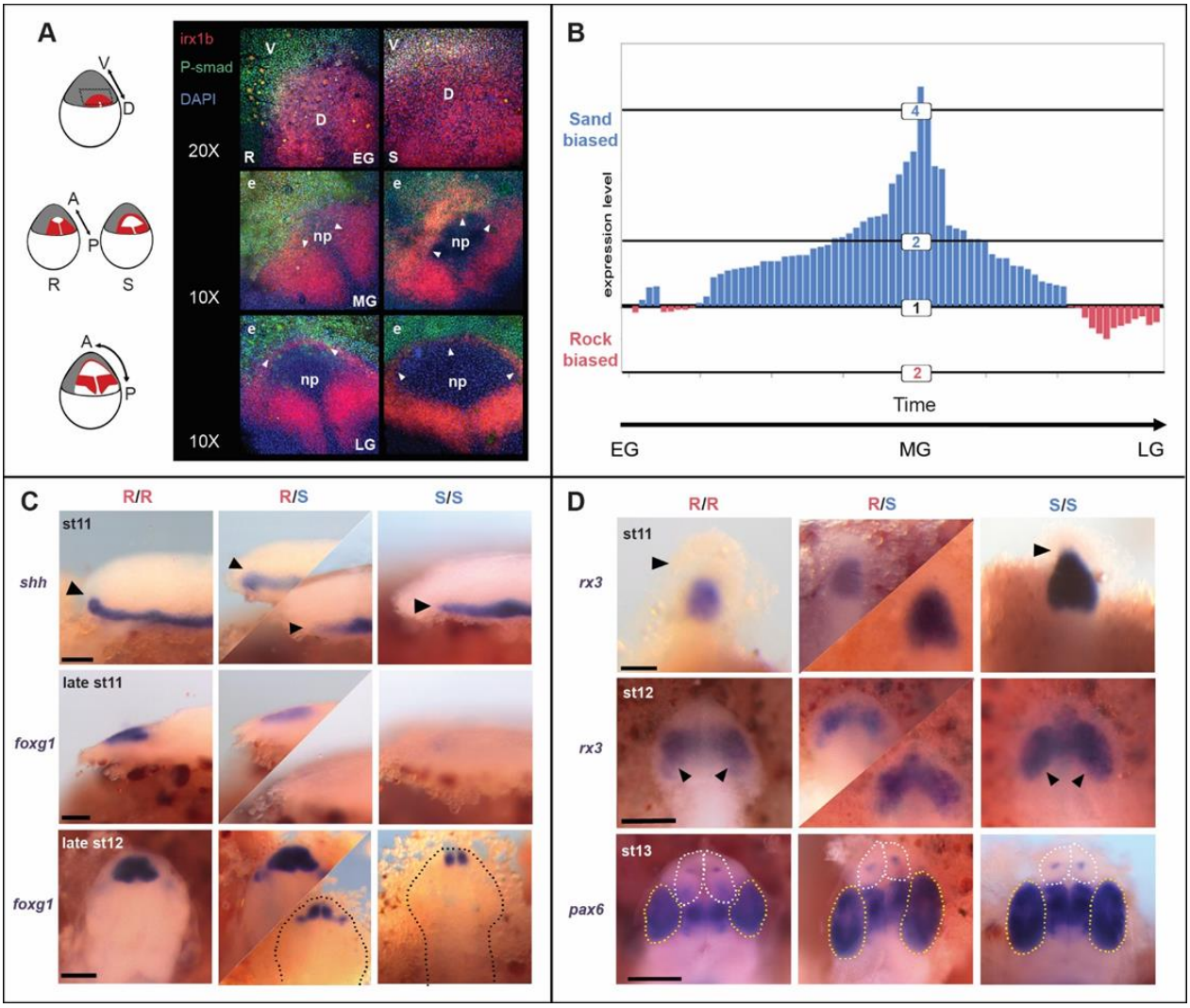

Figure 2: A gastrula-stage map of forebrain diversification | (A) Double in situ hybridization – immunohistochemistry to visualize *irx1b* expression (red) and BMP [PSMAD] activity (green) across the stages of cichlid gastrulation; DAPI in blue. Three rows represent early, mid and late gastrulation (EG, MG, LG) in embryos of rock- (R) and sand-dwelling (S) species. Sand-dwellers show expanded *irx1* expression in the dorsal portion of the embryo at EG, expanded *irx1b* expression in the anterior domain at MG (arrowheads) and clear PSMAD activity from the developing neural plate (np) earlier in LG (arrowheads). e=epidermis. Schematics at left show *irx1b* expression domains in red, on cartoons of cichlid embryos. (B) Relative expression of rock- (red) and sand- (blue) *irx1b* alleles, sampled from 74 heterozygous rock X sand F_2 embryos, across the stages of gastrulation. F_2 embryos were sampled at stage 9 (gastrulation). Because Malawi cichlid species are maternal mouthbrooders and eggs are fertilized in batches per brood, each

854 brood's embryos vary in timing of fertilization by up to 4h. Embryos within broods can
855 therefore be sub-staged in gastrulation (see methods). Each bar on the plot represents
856 the relative allelic expression of sand- and rock- *irx1b* in a heterozygous F_2 individual.
857 Quantification of allele-specific expression (ASE) shows that levels are sand-biased, and
858 that this effect is strongest in MG. (C) in situ hybridization of *shh* and *foxg1*, during neurula
859 stages, showing development of the telencephalon in rock- X sand- F_2 embryos, indexed
860 for *irx1b* genotype. F_2 individuals homozygous for rock- *irx1b* alleles (R/R) show a more
861 dorsal progression of *shh* expression (black arrowheads), an earlier and a larger
862 expression domain of the telencephalon marker *foxg1*. The top two rows are lateral views;
863 bottom row is a dorsal view. Dotted lines demarcate the outline of the embryo in dorsal
864 view. Heterozygous individuals exhibit greater variation in expression domains (middle
865 columns), indicating that genetic factors other than variants in *irx1b* contribute to this
866 phenotype. (D) in situ hybridization for *rx3* and *pax6*, during neurula stages, chart the
867 development of the eye field in rock- X sand- F_2 embryos indexed for *irx1b* genotypes. F_2
868 individuals homozygous for sand- *irx1b* alleles (S/S) show larger domains of *rx3* (black
869 arrowheads) and larger eyes (*pax6*, also marked by yellow dotted line), but smaller
870 telencephala (white dotted line). All panels are dorsal views. Heterozygous individuals
871 exhibit greater variation in expression domains (middle columns), indicating that genetic
872 factors other than variants in *irx1b* contribute to this phenotype.
873

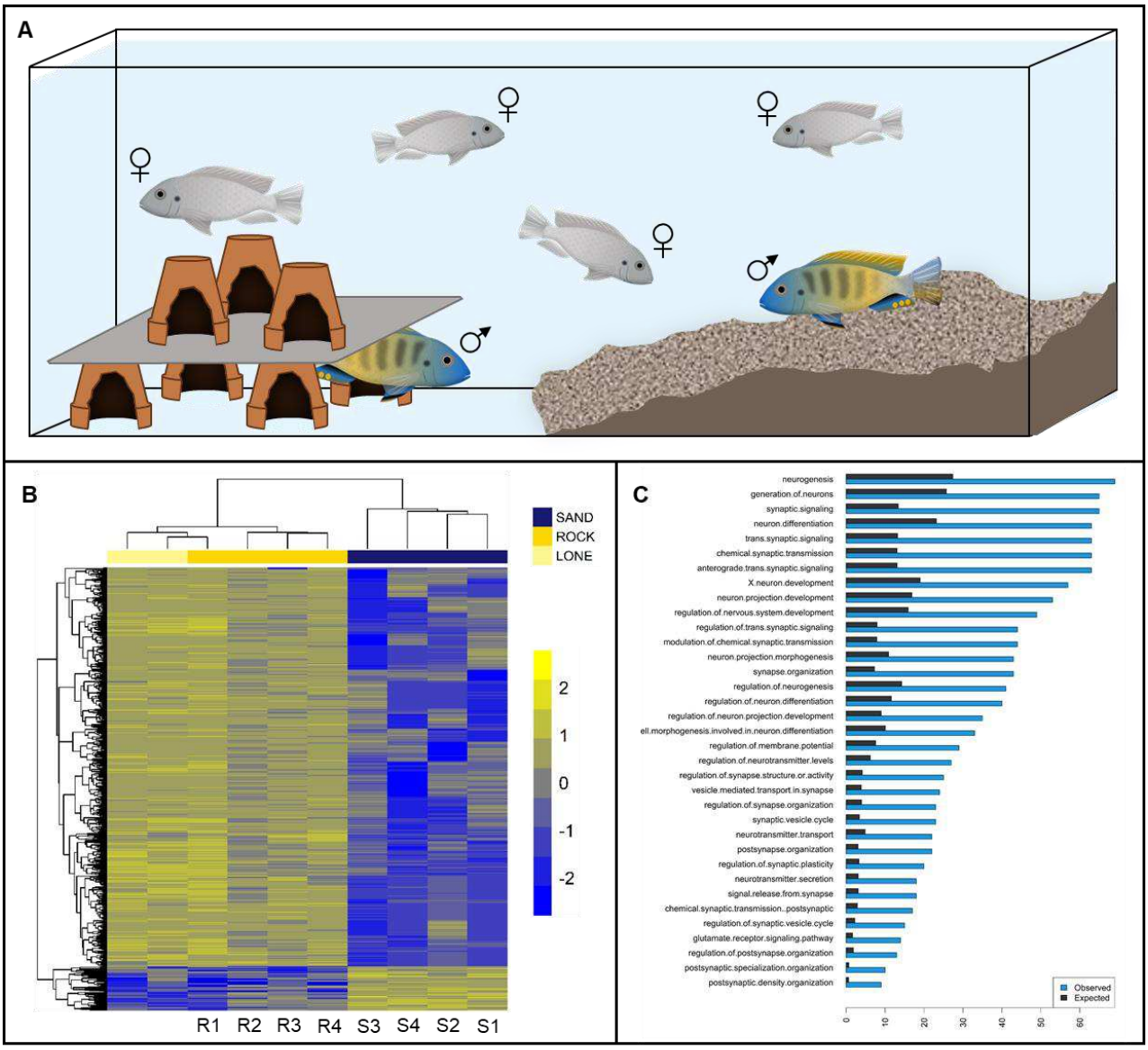

874

875 Figure 3: Genomics of divergent social context | (A) Schematic of the social context
876 behavioral paradigm, in which rock-, sand- and rock- X sand- F_1 hybrids were evaluated.
877 (B) Heatmap of genes differentially expressed in the brains of F_1 males behaving in either
878 rock or sand social contexts. Each row in the heatmap is a gene, each column is an
879 individual. R individuals are socially rock, S individuals are socially sand and the numbers
880 indicate sibling pairs. Two F_1 males were not paired with other males, and courted
881 females over the rock habitat (lone). All other F_1 males (n=8) were introduced to the
882 testing arena in dyads. Notably, male brain gene expression clusters by social context
883 and not fraternal relationships. (C) Gene Ontology (GO) Biological Process terms that

884 show greater than expected overlap between (i) genes differentially expressed in the
885 brains of social rock- vs. social sand- males and (ii) genes that are differentiated in the
886 genomes of rock- vs sand- species groups.

887

888 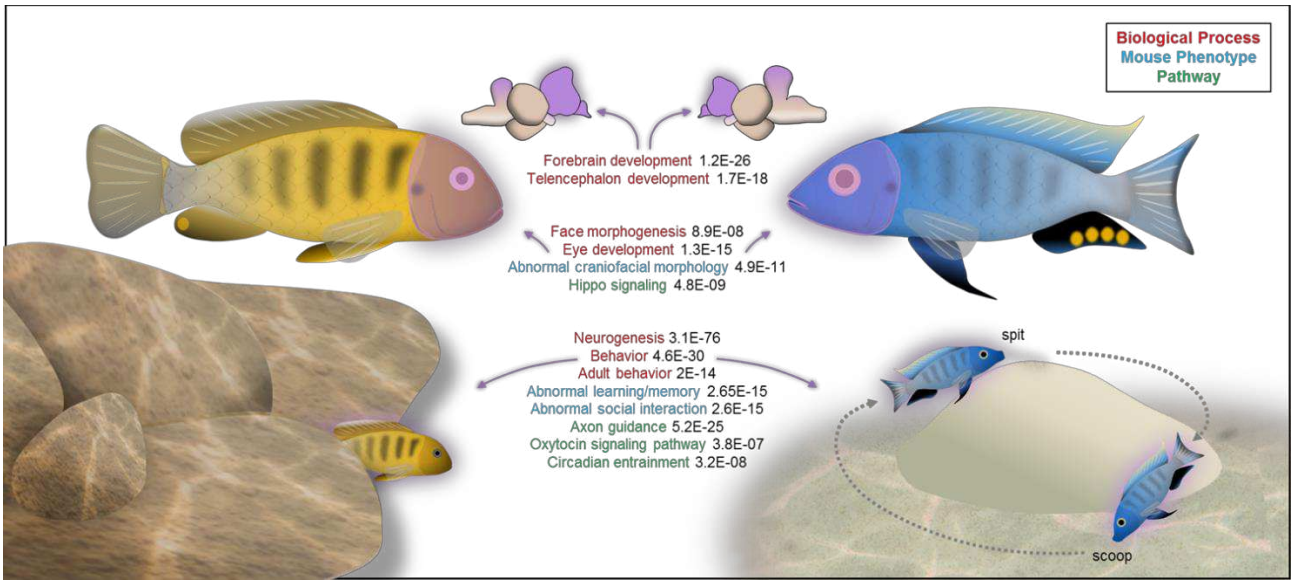

889 Figure 4: Genome-enabled discovery of evolutionary change in morphology and behavior.
890 | Summary cartoon synthesizing significant enrichment categories that differentiate the
891 genomes of rock- vs. sand-dwelling Malawi cichlids. Strong and consistent enrichment of
892 craniofacial, neural and behavioral categories motivated follow-on experiments in early
893 brain development (Figure 2) and adult social behavior (Figure 3).

Figures

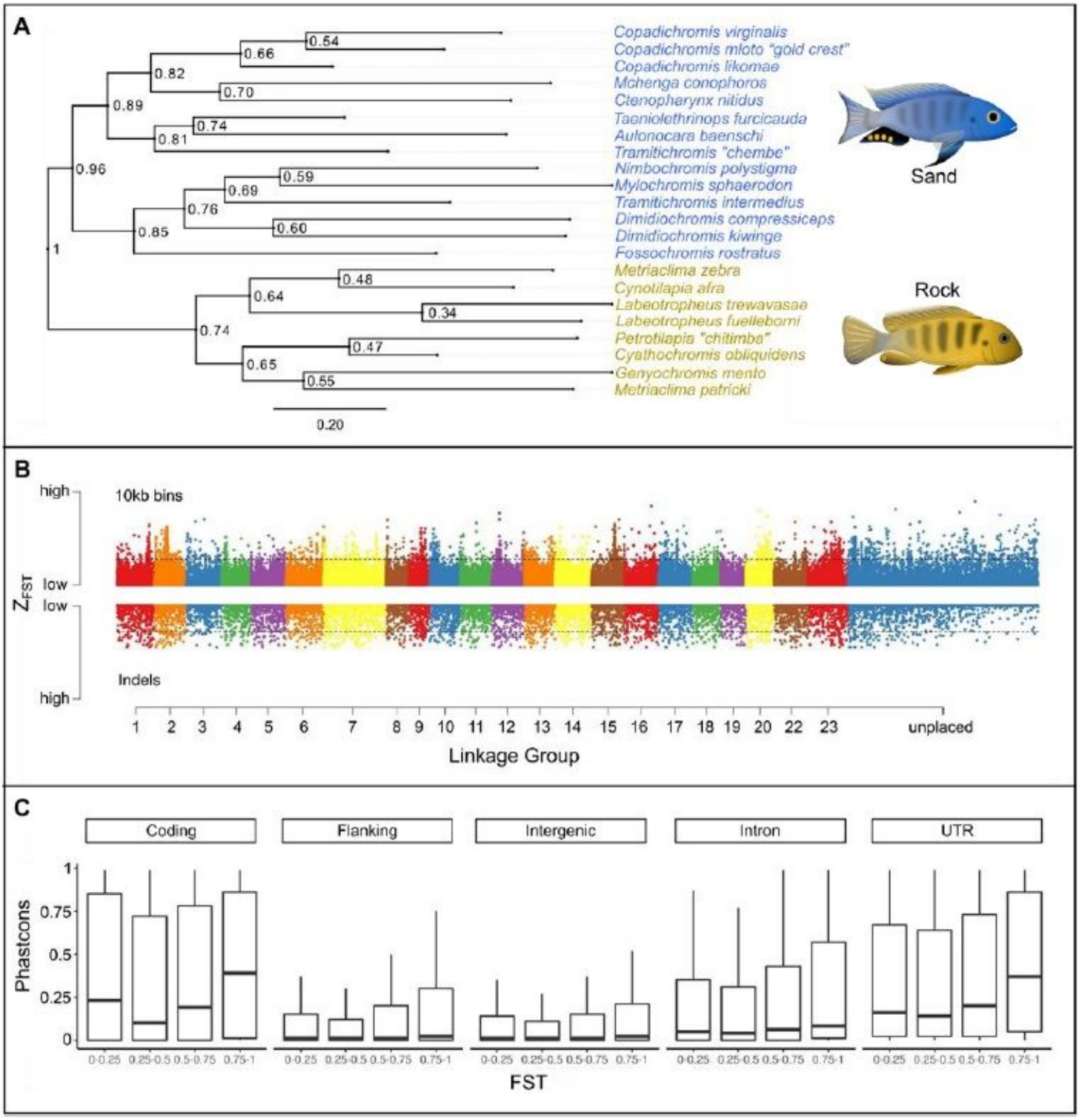

Figure 1

The genomic substrate for rock vs. sand evolution | (A) A maximum likelihood phylogeny of eight rock- and fourteen sand-dwelling species, based on variable sites(informative SNP and InDels) identified throughout the genome. “Sand” species contain representatives of the lineages “shallow benthic, deep

benthic and utaka" from 28, while the "rock" species correspond to the "mbuna" lineage. (B) A plot of Z-FST (FST normalized using Fisher's Z-transformation) across the genome, plotting genomic divergence between rock- vs. sand-dwelling groups. Single nucleotide polymorphisms (SNPs) summed over 10kb bins and insertion-deletion mutations (InDels) are shown on the same scale. Numbers along the x-axis refer to linkage groups (i.e., chromosomes) and threshold lines indicate 2.5% FDR. (C) Evolutionary conservation (PhastCons) scores were calculated for each nucleotide across the genome, subdivided by genome annotation and plotted by bins of increasing FST. The PhastCons score for each genome category is significantly higher for increasing bins of FST (Wilcoxon rank sum p value < 2e-16).

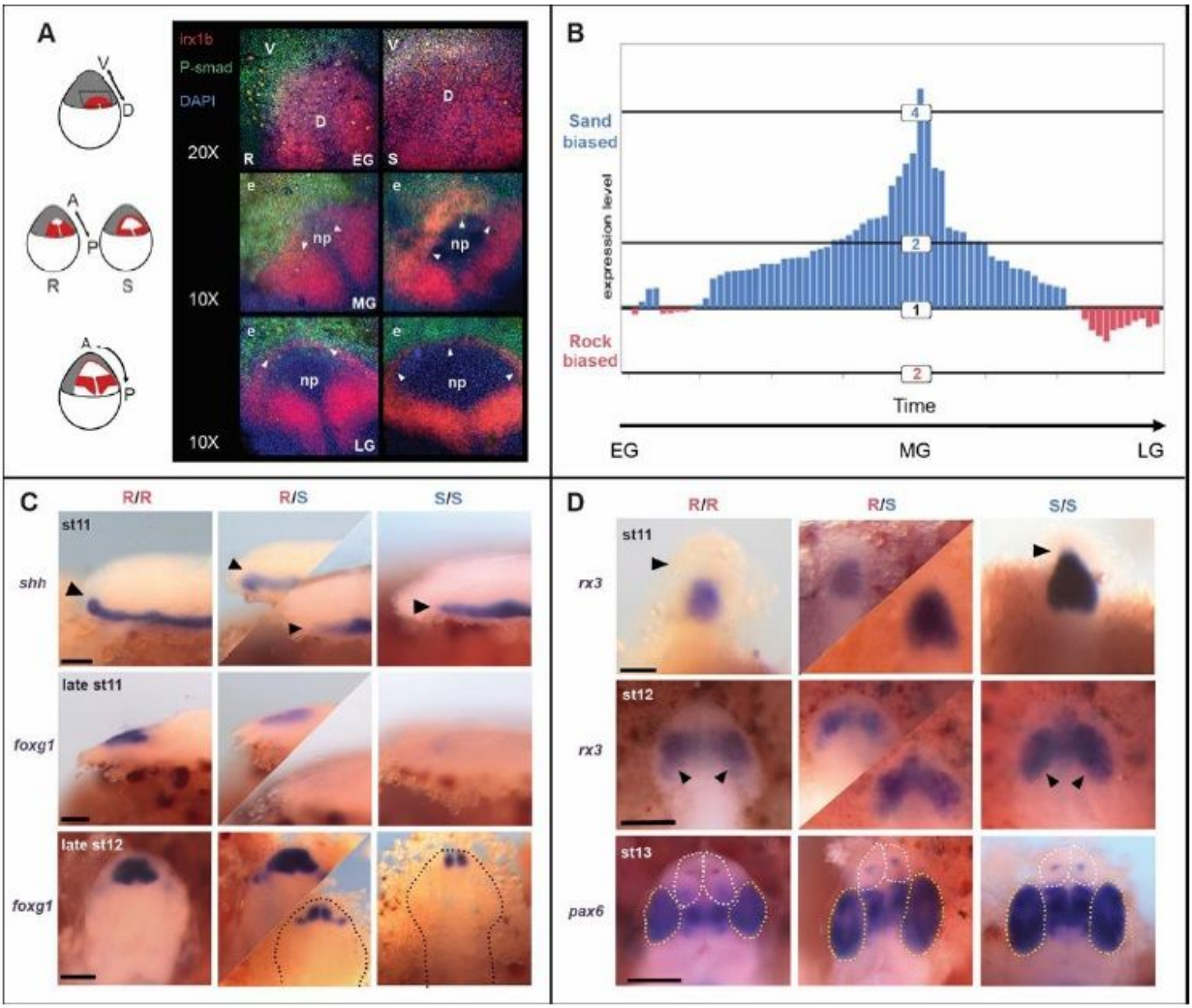

Figure 2

A gastrula-stage map of forebrain diversification | (A) Double in situ hybridization – immunohistochemistry to visualize irx1b expression (red) and BMP [PSMAD] activity 8(green) across the stages of cichlid gastrulation; DAPI in blue. Three rows represent early, mid and late gastrulation (EG, MG,

LG) in embryos of rock- (R) and sand-dwelling (S) species. Sand-dwellers show expanded irx1 expression in the dorsal portion of the embryo at EG, expanded irx1b expression in the anterior domain at MG (arrowheads) and clear PSMAD activity from the developing neural plate (np) earlier in LG (arrowheads). e=epidermis. Schematics at left show irx1b expression domains in red, on cartoons of cichlid embryos. (B) Relative expression of rock- (red) and sand- (blue) irx1b alleles, sampled from 74 heterozygous rock X sand F2 embryos, across the stages of gastrulation. F2 embryos were sampled at stage 9 (gastrulation). Because Malawi cichlid species are maternal mouthbrooders and eggs are fertilized in batches per brood, each brood's embryos vary in timing of fertilization by up to 4h. Embryos within broods can therefore be sub-staged in gastrulation (see methods). Each bar on the plot represents the relative allelic expression of sand- and rock- irx1b in a heterozygous F2 individual. Quantification of allele-specific expression (ASE) shows that levels are sand-biased, and that this effect is strongest in MG. (C) in situ hybridization of shh and foxg1, during neurula stages, showing development of the telencephalon in rock- X sand- F2 embryos, indexed for irx1b genotype. F2 individuals homozygous for rock- irx1b alleles (R/R) show a more dorsal progression of shh expression (black arrowheads), an earlier and a larger expression domain of the telencephalon marker foxg1. The top two rows are lateral views; bottom row is a dorsal view. Dotted lines demarcate the outline of the embryo in dorsal view. Heterozygous individuals exhibit greater variation in expression domains (middle columns), indicating that genetic factors other than variants in irx1b contribute to this phenotype. (D) in situ hybridization for rx3 and pax6, during neurula stages, chart the development of the eye field in rock- X sand- F2 embryos indexed for irx1b genotypes. F2 individuals homozygous for sand- irx1b alleles (S/S) show larger domains of rx3 (black arrowheads) and larger eyes (pax6, also marked by yellow dotted line), but smaller telencephala (white dotted line). All panels are dorsal views. Heterozygous individuals exhibit greater variation in expression domains (middle columns), indicating that genetic factors other than variants in irx1b contribute to this phenotype.

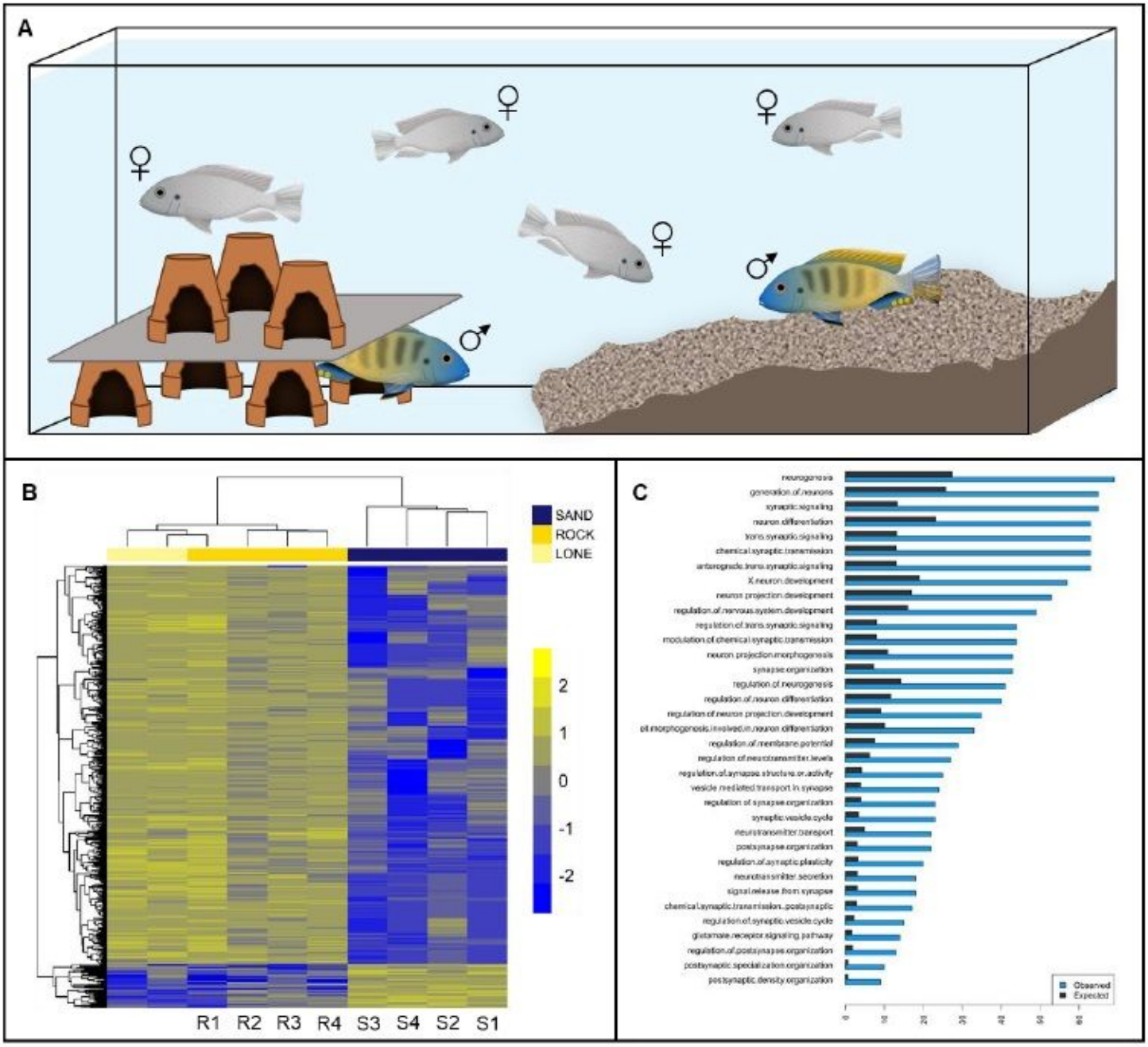

Figure 3

Genomics of divergent social context | (A) Schematic of the social context behavioral paradigm, in which rock-, sand- and rock- X sand- F1 hybrids were evaluated. (B) Heatmap of genes differentially expressed in the brains of F1 males behaving in either rock or sand social contexts. Each row in the heatmap is a gene, each column is an individual. R individuals are socially rock, S individuals are socially sand and the numbers indicate sibling pairs. Two F1 males were not paired with other males, and courted females over the rock habitat (lone). All other F1 males (n=8) were introduced to the testing arena in dyads. Notably, male brain gene expression clusters by social context and not fraternal relationships. (C) Gene Ontology (GO) Biological Process terms that show greater than expected overlap between (i) genes differentially

expressed in the brains of social rock- vs. social sand- males and (ii) genes that are differentiated in the genomes of rock- vs sand- species groups.

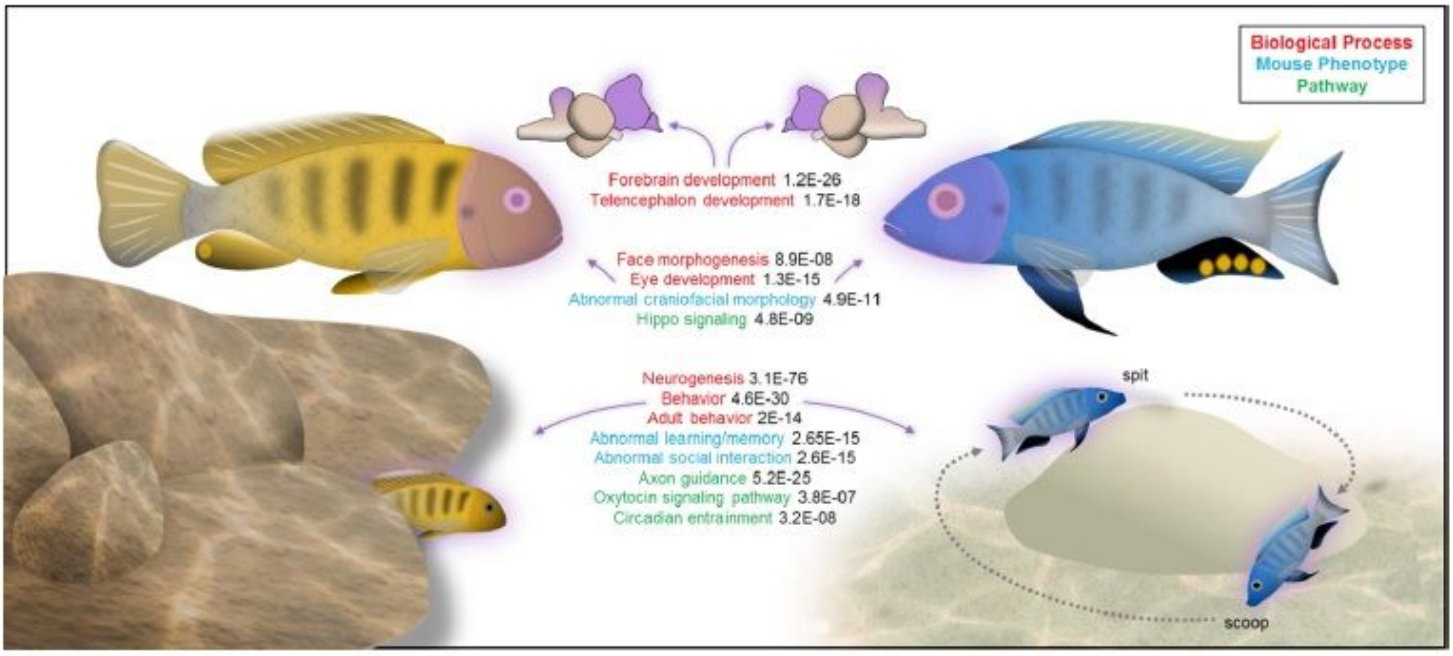

Figure 4

Genome-enabled discovery of evolutionary change in morphology and behavior. | Summary cartoon synthesizing significant enrichment categories that differentiate the genomes of rock- vs. sand-dwelling Malawi cichlids. Strong and consistent enrichment of craniofacial, neural and behavioral categories motivated follow-on experiments in early brain development (Figure 2) and adult social behavior (Figure 3).

Supplementary Files

This is a list of supplementary files associated with this preprint. Click to download.

- SupplementaryTable1Speciesandseqcharacteristics.xlsx
- SupplementaryTable2genomewideidentityofenrichmentGAtopfunSFARIenhancers.xlsx
- SupplementaryTable3RNAseqDEG.xlsx
- SupplementaryTable4rocksandversuspitcastle.xlsx
- SupplementaryTable5SamplesforRNAseq.xlsx
- supplementaryinformation.pdf